Terrestrial stilling will continue during the 21st century

Deliang Chen (deliang@gvc.gu.se)
University of Gothenburg https://orcid.org/0000-0003-0288-5618
Kaiqiang Deng
University of Gothenburg
Cesar Azorin-Molina
University of Gothenburg https://orcid.org/0000-0001-5913-7026
Song Yang
Sun Yat-sen University https://orcid.org/0000-0003-1840-8429
Gangfeng Zhang
Beijing Normal University
Lorenzo Minola
University of Gothenburg

Physical Sciences - Article

Keywords: terrestrial stilling (TS), climate change, wind energy

Posted Date: March 10th, 2021

DOI: https://doi.org/10.21203/rs.3.rs-288223/v1

Terrestrial stilling will continue during the 21st century

Kaiqiang Deng[1], Cesar Azorin-Molina[1,2], Song Yang[3,4], Gangfeng Zhang[5,6], Lorenzo Minola[1], Deliang Chen[1*]

Affiliations:

[1]Regional Climate Group, Department of Earth Sciences, University of Gothenburg, Gothenburg, 40530, Sweden

[2]Centro de Investigaciones sobre Desertificación, Consejo Superior de Investigaciones Científicas (CIDE-CSIC), Moncada, Valencia, Spain

[3]School of Atmospheric Sciences and Guangdong Province Key Laboratory for Climate Change and Natural Disaster Studies, Sun Yat-sen University, Zhuhai, Guangdong 519082, China

[4]Southern Marine Science and Engineering Guangdong Laboratory (Zhuhai), Guangdong 519082, China

[5]State Key Laboratory of Earth Surface Processes and Resource Ecology, Beijing Normal University, Beijing 100875, China

[6]Academy of Disaster Reduction and Emergency Management, Ministry of Emergency Management and Ministry of Education, Beijing Normal University, Beijing 100875, China

*__Correspondence__ to: deliang@gvc.gu.se

Abstract: The near-surface wind speed over land has declined in recent decades, a trend known as terrestrial stilling (TS)[1-2]. However, recent studies have indicated a reversal of the TS in the Northern Hemisphere (NH) during the last decade[3-6], triggering renovated interest in the wind speed changes. Here we show that the TS in the NH mid-latitudes will continue in all seasons throughout the 21st century, especially in summer. The recent reversal of TS is most likely a multi-decadal fluctuation related to the Pacific and Atlantic climate variations, rather than a secular trend. A new paradigm of the future TS is further proposed, which is related to an intensified subsidence inversion over the mid-latitudes,

caused by enhanced tropical and subtropical convections. This study reveals the important role of global warming in reducing the near-surface wind speed on long time scales. The continuing TS means a long-term strategy for wind energy production needs to be developed, particularly for the NH mid-latitude countries.

Main

Both observations and model simulations show that the global near-surface (10-m) wind speed (NWS) over land has declined in the recent decades[7-9]. This phenomenon is termed terrestrial stilling (TS), and has been widely reported across the world, including in Australia[10-11], Europe[12-13], East Asia[14-15], and North America[16-17]. TS can cause great socio-economic and environmental impacts. For example, the slowdown of NWS may reduce surface evaporation and thus affect the hydrological cycle[8,18]. The stilling air also hinders air pollution dispersion, promoting the accumulation of harmful pollutants near emission sources[19-20]. Moreover, as wind power is one of the fastest-growing renewable energy sources and provides an increasing share of electricity[21-22], declining wind speed is likely to exert major impacts on the energy industry. Therefore, it is important to improve our understanding of the past and future NWS changes.

After the TS was recognized[7-9], new findings with regard to the changes in NWS emerged, raising a few key questions that remain to be answered. For example, an increasing number of studies have indicated that the declined NWS has started to recover since the 2000s in Saudi Arabia[3], South Korea[4], China[6], and many other regions in the Northern Hemisphere (NH)[5]. However, it is unclear whether the recent TS reversal is merely a multi-decadal fluctuation or a secular trend that will continue in the future. The other issue is associated with the inconsistent changes between the surface and upper-level winds. Contrary to the NWS, the wind speed in the upper troposphere (e.g., at 200 hPa) has strengthened over recent decades[23]. Previous studies have mainly attributed the surface TS to increased surface roughness (e.g., Earth's greening and urbanization)[23-25] and uneven regional warming[26-28]. Nevertheless, if the surface roughness has dominated the NWS changes, the strongest decreasing trend in wind speed would be expected to appear at the surface level. However, the wind speed in the lower troposphere (below

500hPa) has declined more rapidly at higher altitudes than at the surface[11,29]. Moreover, if the uneven warming had caused the wind speed changes in the past decades, then according to the thermal wind equation, the corresponding reduction in the NH equator-to-pole temperature gradient should have led to weakened westerly jets in the upper troposphere; however, this contradicts observed strengthening of upper-tropospheric winds[23]. In summary, the existing theories are not sufficient to explain the changes in the upper- and lower-troposphere winds.

In this study, we proposed a new mechanism which is able to explain not only the continuing surface TS but also the changes in the upper winds, based on in-situ observations from the Global Surface Summary of the Day database[30] and simulations from the Coupled Model Inter-comparison Project - Phase 6 (CMIP6) models[31]. The CMIP6 models used in this study are listed in Table S1. They include 20 climate models that produced historical simulations for the period 1850–2014, and were extended by four different Shared Socioeconomic Pathway (SSP) scenarios (i.e. SSP126, SSP245, SSP370, and SSP585) for the period 2015–2099. Detailed information on the observed and simulated datasets is presented in Supplementary Information.

Annual NWS changes during the 21st century

Figures 1a and 1b show the observed and simulated spatial distribution of the climatology (1981–2010) of annual NWS. The CMIP6 multiple-model mean has fairly reproduced the distributions and magnitudes of the observed NWS, with a correlation coefficient of +0.85 between the two spatial patterns. When comparing NWS between 2070–2099 and 1981–2010 in Figs. 1c-f, the NWS in mid-to-high latitudes is found to weaken by the end of the 21st century under all scenarios. In contrast, the NWS in the subtropical regions will intensify in future warming climate. More specifically, as seen from Fig. 1g, decreases in NWS are mainly found at latitudes 20°N–70°N, while the increases occur in latitudes 0°–20°N. In general, both the mid-latitude and subtropical NWS changes are larger under higher SSP scenarios, indicating that enhanced future global warming will likely force stronger trends in the NWS.

The time series of annual NWS averaged over the mid-latitude land surface (20°N–

70°N/0°–358°E) for 1979–2099 are shown in Fig. 1h. The NWS in the NH mid-latitudes will experience declining trends under all SSP scenarios. In particular, the decreases in NWS become the greatest under the SSP585 scenario forcing. Opposite to the decrease in mid-latitude NWS, the NWS over the subtropical region was projected to strengthen continuously to 2099, with the largest increasing trends in the SSP585 scenario level (Fig. S1). While the CMIP6 models have accurately simulated the TS in the NH mid-latitudes during 1979–2010, we note that they have underestimated the recent reversal of the TS since around 2010.

Previous studies have suggested that the dominant modes in the Pacific and Atlantic oceans could explain the TS reversal[3,5]. To better understand why the models have underestimated the observed TS reversal, we divide the 20 models into two groups and examine their performances in simulating the Pacific Decadal Oscillation (PDO) and the Atlantic Multi-decadal Oscillation (AMO). As seen from Fig. S2, the first group includes 9 models that have generally reproduced increasing trends in NWS over 2010–2030, i.e. the TS reversal; the other group comprises the 11 models that simulated persistently decreasing trends during 2010–2030, implying that they cannot capture the recent reversal phenomenon. As seen from the subplot in Fig. S2a, those models that could simulate the TS reversal also projected decreasing trends in mid-latitude NWS over the long term (2010–2099). By comparison, the models without TS reversal simulated more robust decreasing trends of NWS during the 21st century (see subplot in Fig. S2b).

We propose that the models' abilities in simulating the PDO and AMO could affect their simulations of the TS reversal. As shown in Fig. S3a, the observed PDO experienced positive-to-negative (negative-to-positive) phase changes during 1979–2010 (2010–the present). The models with TS reversal accurately simulated the phase changes in PDO during 1979–2020 and projected a shift to positive PDO phases during 2020–2030. Moreover, the models with TS reversal produced a stronger spatial variability in the PDO than the models without TS reversal (Fig. S3b). In addition to the PDO, the observed AMO underwent negative-to-positive (positive-to-negative) phase changes during 1979–2010 (2010–the present) (Fig. S4). The models with TS reversal fairly simulated the decreasing trend in the AMO since the 2010s, which were not reproduced by the models

without TS reversal. The results suggest that the recent recovery of TS is more likely a multi-decadal fluctuation related to the phase changes in PDO and AMO, rather than a secular trend in the future.

Seasonal NWS changes and associated atmospheric circulation

Further analysis reveals that the TS phenomenon appears in all seasons (Fig. 2), but with seasonal differences in its magnitude. For example, the largest decreasing trends of mid-latitude NWS over 2015–2099 appear in boreal summer (Fig. 2b), with the higher SSP scenario levels inducing a stronger slowdown. In contrast, trends during boreal winter are much smaller (Fig. 2d). Along with the slowdown in the mid-latitudes, the subtropical NWS strengthens in most seasons except for the boreal winter (see subplots in Fig. 2). Consistent with the mid-latitude winds, the subtropical winds also show the largest trends in summer, suggesting a possible connection in atmospheric circulations between mid- and lower-latitude regions. In addition, the long-term changes in NWS (both mid-latitudes and subtropics) are closely linked to global warming (Fig. S5): the stronger the greenhouse warming, the larger the NWS trend. The changes in NWS show an almost linear relationship with the global warming intensity especially in summer, suggesting that the persisting global warming could play a crucial role in the future TS.

Figure 3 illustrates the future changes in NWS, precipitation, and vertical winds in different seasons between 2070–2099 and 1981–2010. During boreal summer, regions with weakening NWS occur widely across mid-to-high latitudes (Fig. 3d). During winter, however, decreases in NWS are mostly confined south of 40°N (Fig. 3j). Meanwhile, the subtropical NWS intensifies. In particular, during boreal summer, the NWS over South Asia, East Asia, and West Africa will strengthen remarkably. Notice that these areas are the regions affected by the NH summer monsoon: this indicates that the changes in the NH summer monsoon may affect the NWS in the subtropics and the mid-latitudes.

When looking at changes in precipitation (see the middle panels in Fig. 3), we observe two main spatial features. First one is the increased precipitation over the inter-tropical convergence zone (ITCZ), which is especially prominent in the tropical Pacific. The other appears in the NH subtropical regions, where the monsoon precipitation

is projected to increase considerably in the future. The increase in ITCZ precipitation is projected in all seasons, while the increase in monsoon precipitation mainly occurs during boreal summer. Therefore, during summer, the enhancements of ITCZ and monsoon convection may jointly affect the NWS in the NH mid-latitudes. However, during winter, the ITCZ and monsoon convection are mainly located in the Southern Hemisphere, and would thus affect the NH high-latitude NWS less than they do during the summer. The enhancement of future precipitation would trigger anomalously ascending and descending motions in the troposphere (see the right panels in Fig. 3). In particular, there are two centers of ascending motion: one over the tropical regions, related to the deep ITCZ convection, and the other located over the subtropics, associated with the relatively shallow monsoon convection. The intensified tropical and subtropical rising motions force sinking air over the mid-latitudes.

A new paradigm of the future TS

The anomalous descending motions over the mid-latitudes, due to the enhanced low-latitude convection, could result in an anomalous subsidence inversion in the mid-latitude troposphere, through adiabatic heating. As shown in the left panels of Fig. S6, the mid-latitude air temperatures are projected to increase in the entire troposphere in the future. However, the warming rates are not the same at different levels, which are greatest around the 300-hPa level. The vertical distribution of future air temperature increase reveals the development of a subsidence inversion in the lower troposphere and a strengthened lapse rate above the 300-hPa level. The subsidence inversion during summer is obviously stronger than that during winter, probably due to the enhanced summer monsoon convection.

Under the control of the subsidence inversion, the lower-tropospheric atmosphere becomes more stable, which may suppress surface convergence and reduce the frequency of strong winds, in favor of the persisting TS. Nevertheless, in the upper troposphere, the larger lapse rate would increase the instability in the atmosphere, which strengthens upper tropospheric winds. Indeed, further examination reveals that the zonal wind speed below the 300-hPa level would become weakened in the future, especially during summer

(middle panels of Fig. S6). By comparison, the zonal wind speed above 300 hPa becomes stronger. The vertical profile of the meridional wind speed change is similar to that of zonal wind speed, with reduced (enhanced) meridional wind speed in the lower (upper) troposphere (right panels of Fig. S6). Therefore, the subsidence inversion hypothesis could not only explain the future TS, but also the inconsistent changes in the lower and upper-tropospheric winds.

To summarize, the TS will continue during the 21st century in all four seasons across the NH mid-latitudes under all SSP scenarios, with the strongest decrease during boreal summer. The recent recovery of TS likely reflects a multi-decadal fluctuation related to the phase changes in the PDO and the AMO, rather than a secular trend in the future. Finally, to explain what drives the TS, we propose a new physical mechanism illustrated in Fig. 4. In a future warmer climate, the tropical sea surface temperature would be higher, which enhances the ITCZ convection and intensifies the Hadley cell. Meanwhile, during summer, the NH monsoon rainfall would increase, which induces above-normal upward motions and strengthened NWS in the subtropics. The intensified upward motions over the tropical and subtropical regions force stronger sinking air over the mid-latitudes, causing an anomalous subsidence inversion in the lower troposphere. As a result, the atmosphere becomes more stable and the TS is reinforced.

The continuing TS has important implications for future wind energy development, especially for the NH mid-latitude countries where a large number of wind generators have been installed, such as those in Europe, East Asia, and North America. Moreover, air pollution dispersion over these regions may become more challenging due to the stilling air and the reduced occurrences of windy days. Therefore, a long-term strategy of wind energy development and environmental protection should be considered to reduce the potential economic losses and environmental impacts.

Acknowledgments: We appreciate several helpful discussions with colleagues in the Regional Climate Group at the University of Gothenburg. This study is funded by the Swedish Research Council (VR-2017-03780 and VR-2019-03954), the Ramon y Cajal Fellowship (RYC-2017-22830), the Spanish Ministry of Science, Innovation and

Universities (RTI2018-095749-A-I00), the Second Tibetan Plateau Scientific Expedition and Research Program (Grant 2019QZKK0606), and Swedish MERGE and BECC. The computational resources were provided by the Swedish National Infrastructure for Computing at the National Supercomputer Centre in Sweden.

Author contributions: K.D. and D.C. designed the research and conducted analyses. K.D. wrote the majority of the manuscript content. C.A., S.Y., G.Z. and L.M. contributed to the analysis and writing. All of the authors reviewed the manuscript.

Competing interests: Authors declare no competing interests.

Data availability statement: All datasets used in this study are freely accessible. The wind observations are retrieved from the Global Surface Summary of the Day database (ftp://ftp.ncdc.noaa.gov/pub/data/gsod; last accessed on 1 February 2021). The CMIP6 outputs are downloaded through the portal of the Lawrence Livermore National Laboratory (https://esgf-node.llnl.gov/search/cmip6/; last accessed 1 February 2021).

Code availability statement: All codes and climate indices are available upon request from K.D.

References

1. Duan, K. *et al.* Assessing the roles of terrestrial stilling and solar dimming in land surface drying/wetting across China. *Water* **12,** 1996 (2020).
2. Zeng, Z. *et al.* Global terrestrial stilling: does Earth's greening play a role? *Environ. Res. Lett.* **13,** 124013 (2018).
3. Azorin-Molina, C. *et al.*, Recent trends in wind speed across Saudi Arabia, 1978–2013: A break in the stilling. *Int. J. Climatol.* **38,** e966–e984 (2018).
4. Kim, K., Paik, K. Recent recovery of surface wind speed after decadal decrease: a focus on South Korea. *Clim. Dyn.* **45,** 1699–1712 (2015).
5. Zeng, Z. *et al.*, A reversal in global terrestrial stilling and its implications for wind energy production. *Nat. Clim. Chang.* **9,** 979–985 (2019).
6. Zhang, Z., Wang, K. Stilling and recovery of the surface wind speed based on

observation, reanalysis, and geostrophic wind theory over China from 1960 to 2017. *J. Clim.* **33,** 3989–4008 (2020).

7. McVicar, T. R., Roderick, M. L. Winds of change. *Nat. Geosci.* **3,** 747–748 (2010).
8. McVicar, T. R. *et al.* Global review and synthesis of trends in observed terrestrial near-surface wind speeds: Implications for evaporation. *J. Hydrol.* **416–417,** 182–205 (2012).
9. Torralba, V. *et al.* Uncertainty in recent near-surface wind speed trends: a global reanalysis intercomparison. *Environ. Res. Lett.* **12,** 114019 (2017).
10. McVicar, T. R. *et al.* Wind speed climatology and trends for Australia, 1975–2006: Capturing the stilling phenomenon and comparison with near-surface reanalysis output. *Geophys. Res. Lett.* **35,** L20403 (2008).
11. Troccoli, A. *et al.* Long-term wind speed trends over Australia. *J. Clim.* **25,** 170–183 (2012).
12. Azorin-Molina, C. *et al.* Homogenization and assessment of observed near-surface wind speed trends over Spain and Portugal, 1961–2011. *J. Clim.* **27,** 3692–3712 (2014).
13. Minola, L., *et al.* Homogenization and assessment of observed near-surface wind speed trends across Sweden, 1956–2013. *J. Clim.* **29,** 7397–7415 (2016).
14. Guo, H., *et al.* Changes in near-surface wind speed in China: 1969–2005. *Int. J. Climatol.* **31,** 349–358 (2011)
15. Zha, J. *et al.*, Future projections of the near-surface wind speed over eastern China based on CMIP5 datasets. *Clim. Dyn.* **54,** 2361–2385 (2020).
16. Pryor, S. C. *et al.*, Wind speed trends over the contiguous United States. *J. Geophys. Res. Atmos.* **114,** D14105 (2009).
17. Wan, H., *et al.* Homogenization and trend analysis of Canadian near-surface wind speeds. *J. Clim.* **23,** 1209–1225 (2010)
18. McVicar, T. R. *et al.* Less bluster ahead? Ecohydrological implications of global trends of terrestrial near-surface wind speeds. *Ecohydrol.* **5,** 381–388 (2012).
19. Cai, W. *et al.* Weather conditions conducive to Beijing severe haze more frequent under climate change. *Nat. Clim. Chang.* **7,** 257–262 (2017).

20. Jury, M. R. Meteorology of air pollution in Los Angeles. *Atmos. Pollut. Res.* **11,** 1226–1237 (2020).
21. Dincer, F. The analysis on wind energy electricity generation status, potential and policies in the world. *Renew. Sustain. Energ. Rev.* **15,** 5135–5142 (2011).
22. Kramm G. *et al.* Near-surface wind-speed stilling in Alaska during 1984-2016 and its impact on the sustainability of wind power. *J. Pow. Energ. Engineer.* **7,** 71–124 (2019).
23. Vautard, R. *et al.* Northern Hemisphere atmospheric stilling partly attributed to an increase in surface roughness. *Nat. Geosci.* **3,** 756–761 (2010).
24. Zhang, Z. *et al.* Increase in surface friction dominates the observed surface wind speed decline during 1973–2014 in the Northern Hemisphere lands. *J. Clim.* **32,** 7421–7435 (2019).
25. Wang, J. *et al.* An analysis of the urbanization contribution to observed terrestrial stilling in the Beijing–Tianjin–Hebei region of China. *Environ. Res. Lett.* **15,** 034062 (2020).
26. Francis, J. A., Vavrus, S. J. Evidence linking Arctic amplification to extreme weather in mid-latitudes. *Geophys. Res. Lett.* **39,** L06801 (2012).
27. Barnes, E. A., Screen, J. A. The impact of Arctic warming on the midlatitude jet-stream: Can it? Has it? Will it? *WIRes Clim. Chang.* **6,** 277–286 (2015).
28. Coumou, D. *et al.* The influence of Arctic amplification on mid-latitude summer circulation. *Nat. Commun.* **9,** 2959 (2018).
29. Lin, C. *et al.* Observed coherent trends of surface and upper-air wind speed over China since 1960. *J. Clim.* **26,** 2891–2903 (2013).
30. Smith, A. *et al.* The integrated surface database: Recent developments and partnerships. *Bull. Amer. Meteor. Soc.* **92,** 704–708 (2011).
31. Eyring, V. *et al.* Overview of the Coupled Model Intercomparison Project Phase 6 (CMIP6) experimental design and organization. *Geosci. Model Dev. Discuss.* **8,** 10539–10583 (2016).

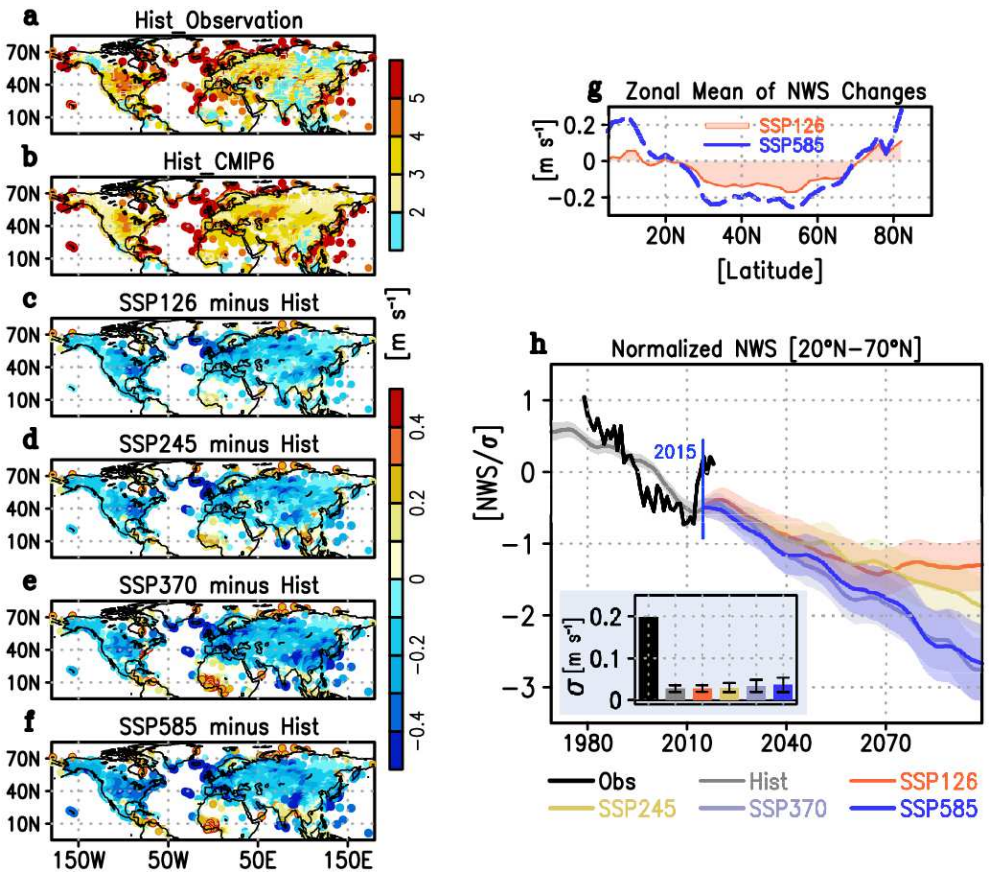

Fig. 1 Annual NWS changes in the 21st century. a-b, Climatological patterns of NWS for 1981–2010 based on observations (**a**) and model simulations (**b**). **c-f**, Differences in simulated NWS between periods 2070–2099 and 1981–2010, driven by SSP126 (**c**), SSP245 (**d**), SSP370 (**e**), and SSP558 (**f**) scenarios during 2070–2099. **g,** Zonal mean of future NWS changes under SSP126 and SSP585 scenarios. The unit for NWS is m s^{-1}. **h,** Time series of NWS averaged over the NH mid-latitudes (20°N–70°N), driven by the historical all forcing during 1979–2014 and the four SSPs during 2015–2099. The NWS time series were normalized based on the mean and standardized deviation (σ) of the NWS over 1981–2010. In the subplot, the bars indicate the σ for observations (black) and historical simulations (grey) during 1981–2010 and for the future projections (colors) during 2015–2099. Shadings in (**h**) denote the inter-model spreads, defined as one standard deviation of the individual models' departures from the 20 model mean. All time series are 10-year running means. The vertical blue line indicates the year 2015.

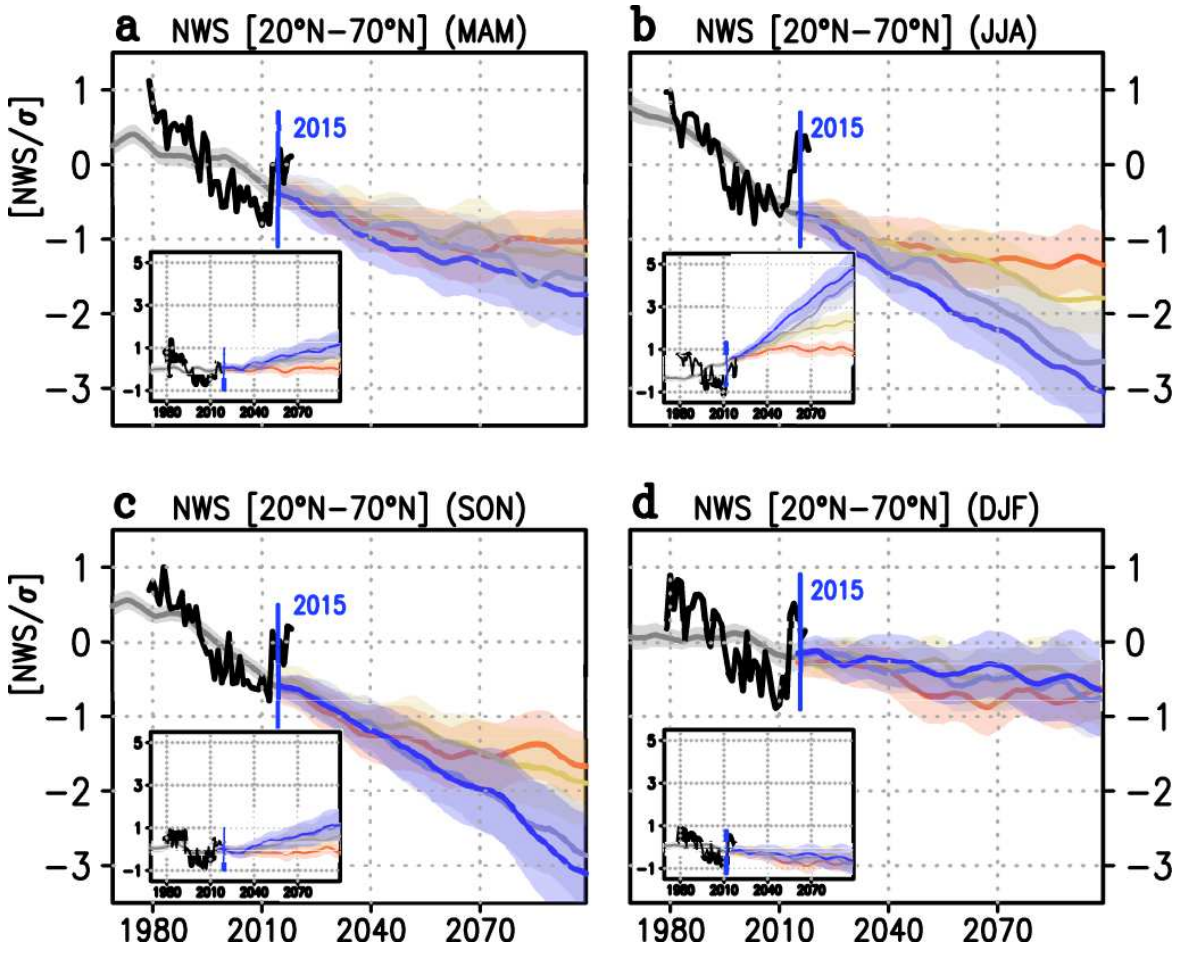

Fig. 2 Seasonal NWS changes in mid-latitudes and subtropics. a-d, Similar to **Fig. 1h**, but for the NWS averaged over the NH mid-latitudes (20°N–70°N) in boreal spring (MAM: March-April-May) (**a**), summer (JJA: June-July-August) (**b**), autumn (SON: September-October-November) (**c**), and winter (DJF: December-January-February) (**d**). The subplots within each panel are for the NWS averaged over the subtropics (0°–20°N). Shadings denote the inter-model spreads, defined as one standard deviation of the individual models' departures from the 20 model mean. All time series are 10-year running means. The vertical blue line indicates the year 2015.

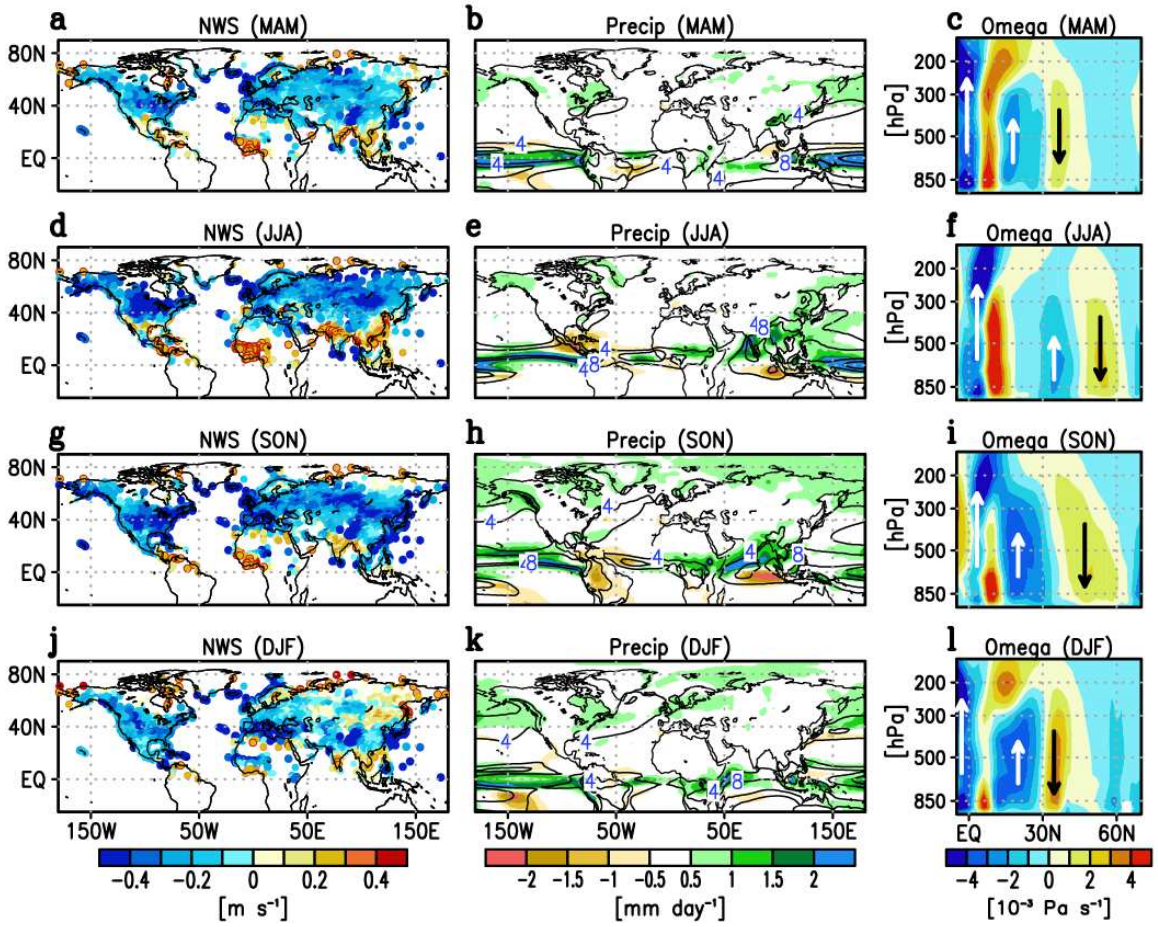

Fig. 3 Future changes in NWS, precipitation and vertical winds for the four seasons. **a**-**c**, Differences (shading) in simulated NWS (**a**), precipitation (**b**), and vertical winds (**c**) between the periods 2070–2099 and 1981–2010 for the NH spring and under the SSP585 scenario. The units for NWS, precipitation, and vertical wind are m s^{-1}, mm day^{-1}, and 10^{-3} Pascal s^{-1}, respectively. **d**-**f**, **g**-**i** and **j**-**l,** Similar to **a**-**c**, except for summer, autumn, and winter, respectively. Contours in the precipitation panels (middle) denote the climatology in 1981–2010. Vectors in the omega panels (right) indicate the upward (white) or downward (black) air motions.

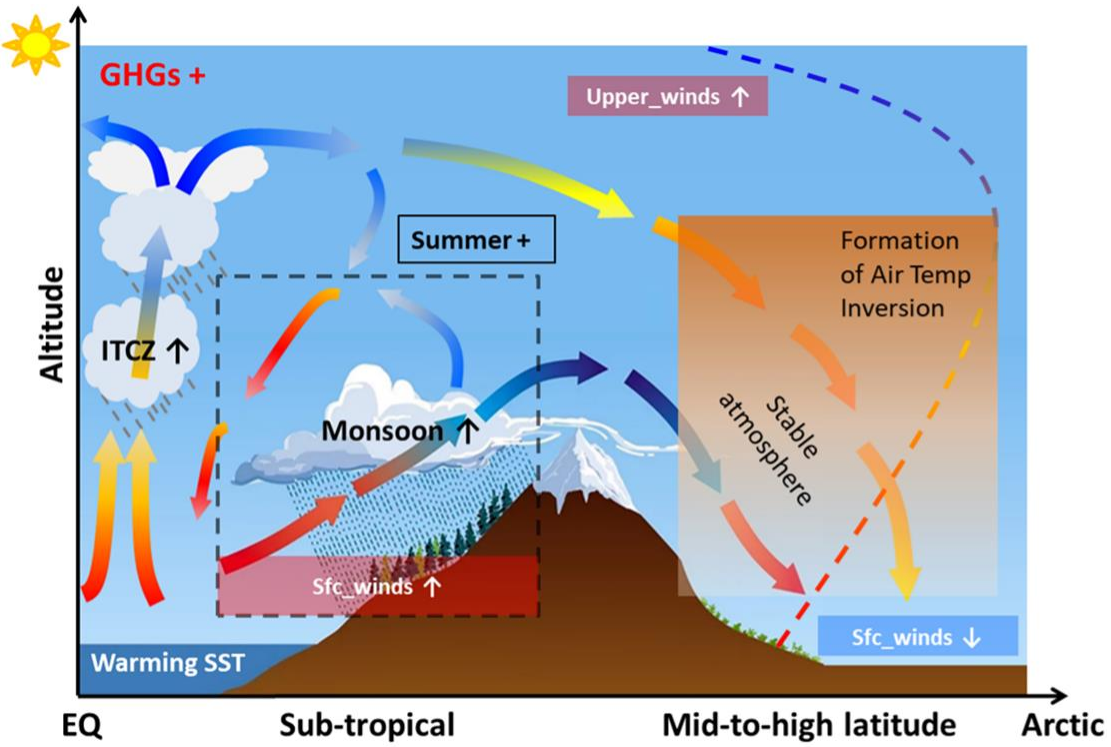

Fig. 4 Schematic diagram illustrating the physical mechanisms for the TS. Vectors indicate changes in the atmospheric circulation. Intensified upward motions over the tropical and subtropical regions, due respectively to the enhanced ITCZ and monsoon convections, would enhance sinking motions over the NH mid-latitudes. Dashed curve over the mid-to-high latitudes denote the vertical profile of future air temperature changes, reflecting an intensified subsidence inversion in the lower troposphere and strengthened lapse rate in the upper troposphere. As a result, the atmosphere in lower (upper) troposphere becomes more stable (unstable), which is conducive to the TS (the strengthening of upper-troposphere winds).

Figures

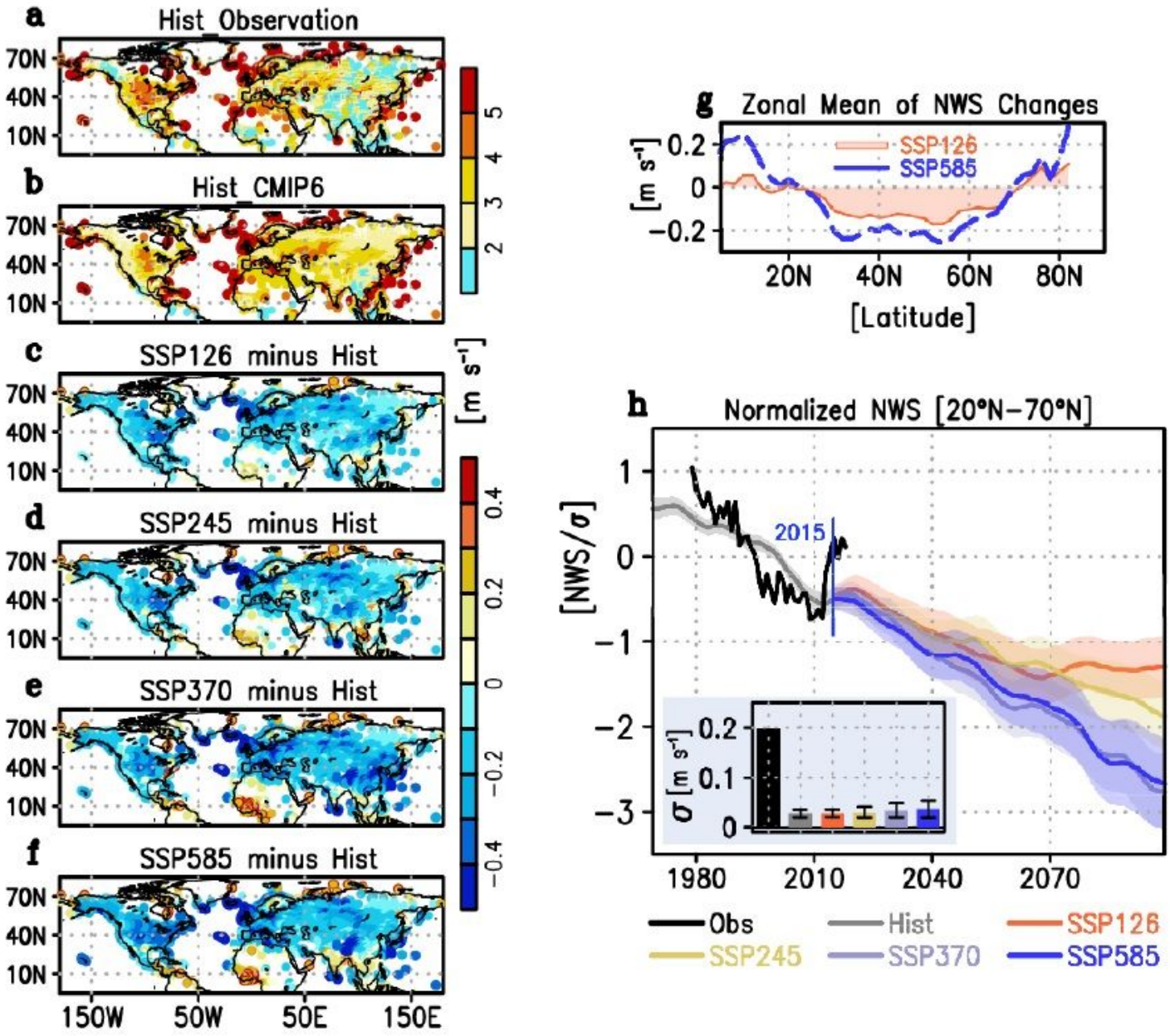

Figure 1

Annual NWS changes in the 21st century. a-b, Climatological patterns of NWS for 1981–2010 based on observations (a) and model simulations (b). c-f, Differences in simulated NWS between periods 2070–2099 and 1981–2010, driven by SSP126 (c), SSP245 (d), SSP370 (e), and SSP558 (f) scenarios during 2070–2099. g, Zonal mean of future NWS changes under SSP126 and SSP585 scenarios. The unit for NWS is m s-1. h, Time series of NWS averaged over the NH mid-latitudes (20°N–70°N), driven by the historical all forcing during 1979–2014 and the four SSPs during 2015–2099. The NWS time series were normalized based on the mean and standardized deviation (σ) of the NWS over 1981–2010. In the subplot, the bars indicate the σ for observations (black) and historical simulations (grey) during 1981–

2010 and for the future projections (colors) during 2015–2099. Shadings in (h) denote the inter-model spreads, defined as one standard deviation of the individual models' departures from the 20 model mean. All time series are 10-year running means. The vertical blue line indicates the year 2015. Note: The designations employed and the presentation of the material on this map do not imply the expression of any opinion whatsoever on the part of Research Square concerning the legal status of any country, territory, city or area or of its authorities, or concerning the delimitation of its frontiers or boundaries. This map has been provided by the authors.

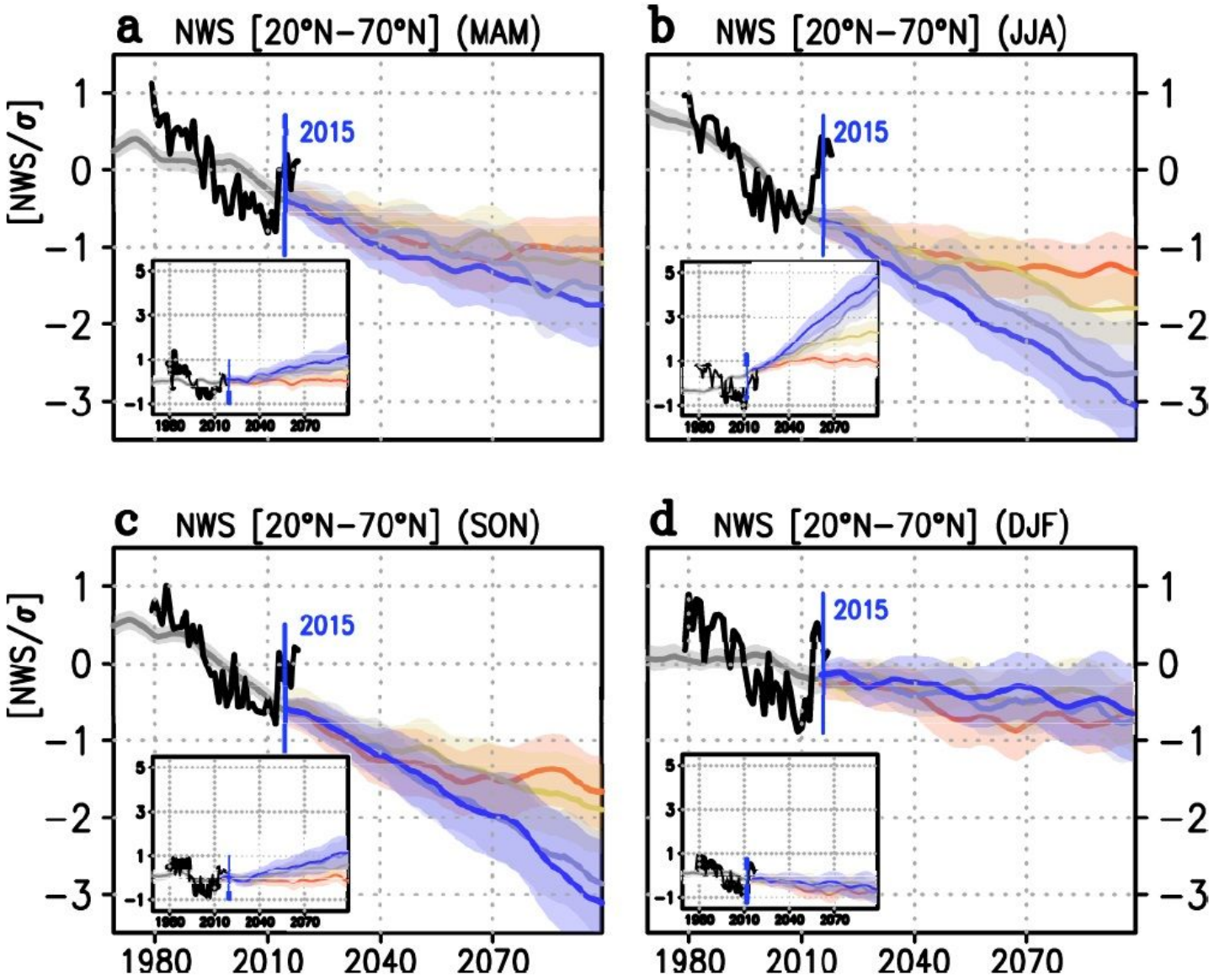

Figure 2

Seasonal NWS changes in mid-latitudes and subtropics. a-d, Similar to Fig. 1h, but for the NWS averaged over the NH mid-latitudes (20°N–70°N) in boreal spring (MAM: March-April-May) (a), summer (JJA: June-July-August) (b), autumn (SON: September-October-November) (c), and winter (DJF: December-January-February) (d). The subplots within each panel are for the NWS averaged over the subtropics (0°–20°N). Shadings denote the inter-model spreads, defined as one standard deviation of the individual models'

departures from the 20 model mean. All time series are 10-year running means. The vertical blue line indicates the year 2015.

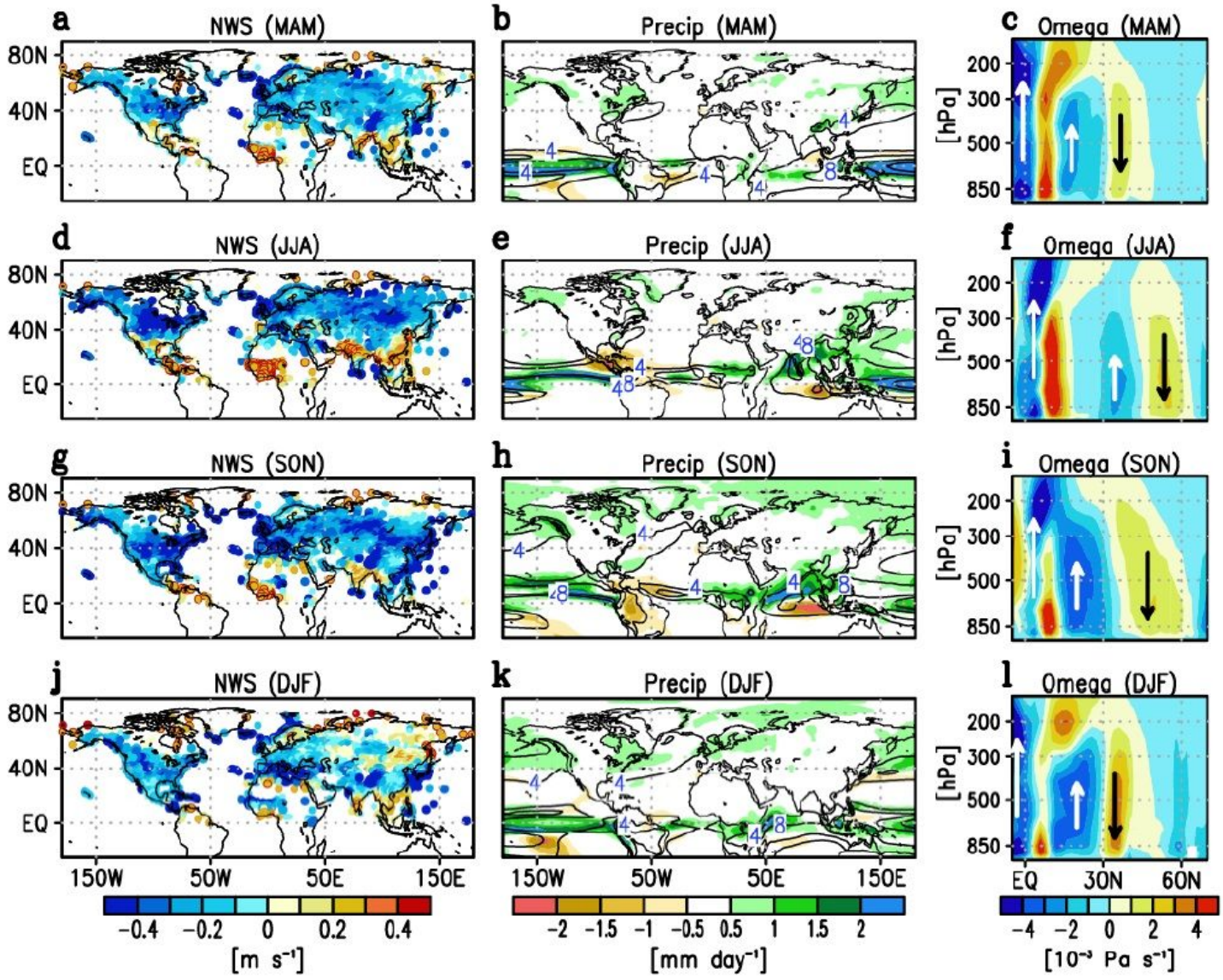

Figure 3

Future changes in NWS, precipitation and vertical winds for the four seasons. a-c, Differences (shading) in simulated NWS (a), precipitation (b), and vertical winds (c) between the periods 2070–2099 and 1981–2010 for the NH spring and under the SSP585 scenario. The units for NWS, precipitation, and vertical wind are m s-1, mm day-1, and 10-3 Pascal s-1, respectively. d-f, g-i and j-l, Similar to a-c, except for summer, autumn, and winter, respectively. Contours in the precipitation panels (middle) denote the climatology in 1981–2010. Vectors in the omega panels (right) indicate the upward (white) or downward (black) air motions. Note: The designations employed and the presentation of the material on this map do not imply the expression of any opinion whatsoever on the part of Research Square concerning the legal status of any country, territory, city or area or of its authorities, or concerning the delimitation of its frontiers or boundaries. This map has been provided by the authors.

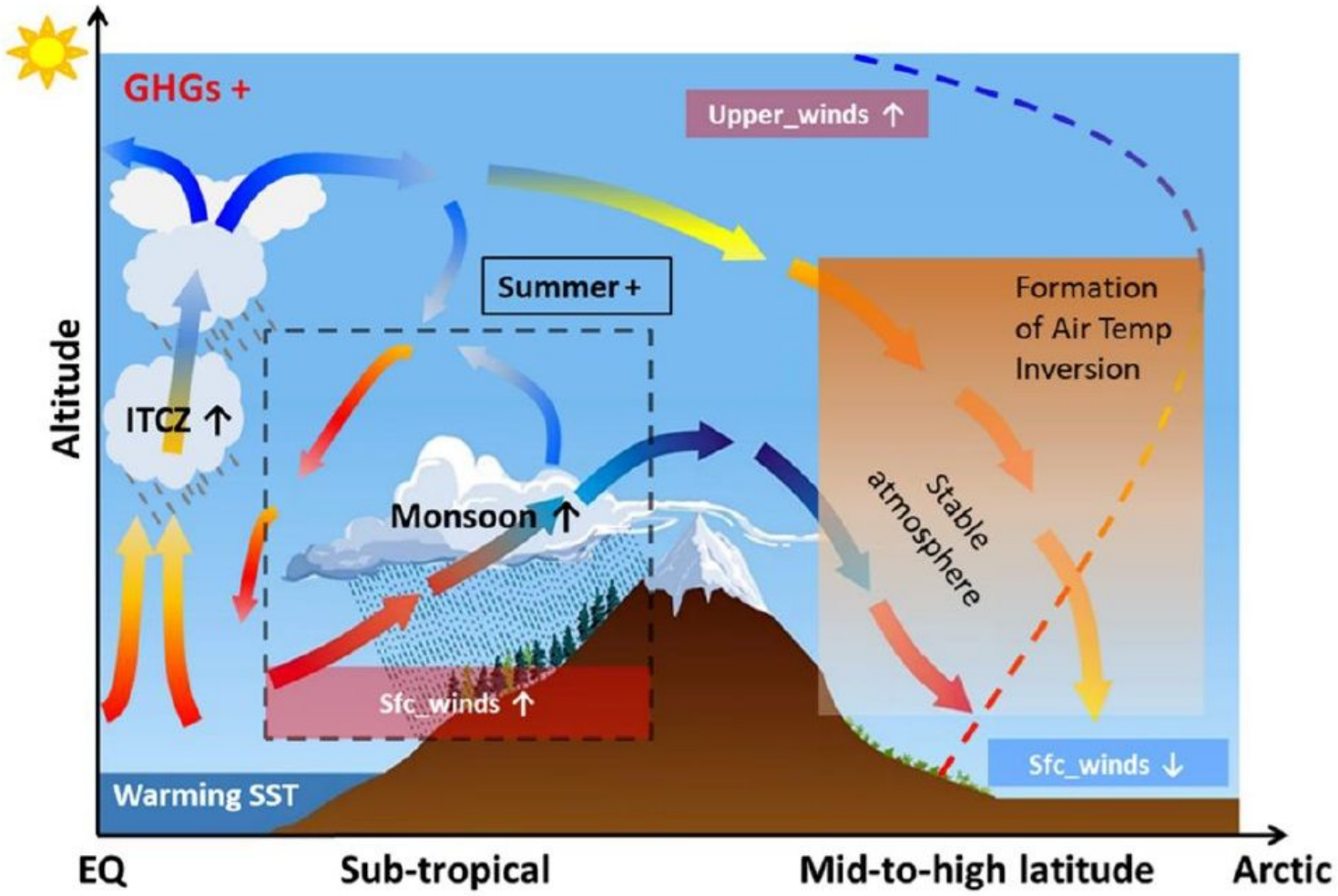

Figure 4

Schematic diagram illustrating the physical mechanisms for the TS. Vectors indicate changes in the atmospheric circulation. Intensified upward motions over the tropical and subtropical regions, due respectively to the enhanced ITCZ and monsoon convections, would enhance sinking motions over the NH mid-latitudes. Dashed curve over the mid-to-high latitudes denote the vertical profile of future air temperature changes, reflecting an intensified subsidence inversion in the lower troposphere and strengthened lapse rate in the upper troposphere. As a result, the atmosphere in lower (upper) troposphere becomes more stable (unstable), which is conducive to the TS (the strengthening of upper-troposphere winds).

Supplementary Files

This is a list of supplementary files associated with this preprint. Click to download.

- SupplementaryInformation.pdf